http://dx.doi.org/10.1109/PESW.2002.985240

Hettiwatte, S.N., Wang, Z.D., Crossley, P.A., Darwin, A. and Edwards, G. (2002) Experimental investigation into the propagation of partial discharge pulses in transformers. In: IEEE Power Engineering Society Winter Meeting, 27 - 31 January, New York, pp 1372-1377.

Experimental Investigation into the Propagation of Partial Discharge Pulses in Transformers

S. N. Hettiwatte, Z. D. Wang, *MIEEE*, P. A. Crossley, *MIEEE*, A. Darwin, *SMIEEE* and G. Edwards

***Abstract*— An experimental investigation into the propagation behaviour of partial discharge (PD) pulses in a continuous disc type 6.6kV transformer winding is described in this paper. PD pulses were injected into the winding using a calibrator and the resulting current signals at the line and neutral end terminals measured using wide band current transformers. The location of the troughs (or zeros) in the frequency spectra of the measured signals change in accordance with the position of the injected pulse. The crests (or poles) in the spectra convey information about the resonance frequencies of the winding and are not affected by the position of the injected pulse. The measured spectra are compared with the spectra generated by a simulation model and although differences exist the overall shape and location of the poles and zeros are similar.**

***Index Terms*—Adaptive Filters, Partial Discharges, Power Transformers, Signal Processing and Simulation.**

I. Introduction

PROPAGATION of partial discharge (PD) pulses in a transformer winding are investigated using an experimental test system and a simulation model based on multi-conductor transmission line theory. The test system is used to validate the simulation model and investigate the effect on the frequency spectra of the line and neutral-end current signals of injecting a PD pulse at different points on the winding. The crests (or poles) in the spectra of the simulated signals [1] always occur at fixed frequencies and are not affected by the location of the PD. The troughs (or zeros) in the simulated line-end spectra increase in frequency, and those in the neutral-end reduce in frequency, as the PD moves away from the line-end. Such features can be used to locate the source of a PD in a transformer [2].

PD pulses were injected into different turns of the winding and the resulting current signals at the line and neutral-end terminals recorded. The spectra of the signals were analysed and compared with those generated by a simulator configured to model the test winding with a PD at the same location. The shape of the spectra and the location of the poles and zeros are similar but differences exist due to noise, inaccuracies in the simulation model and measurement system limitations.

This work was technically and financially supported by Alstom, Edison Mission, National Grid Company, Open University of Sri Lanka and UMIST.
Sujeewa Hettiwatte is a Lecturer at the Open University, Sri Lanka studying for PhD degree at UMIST, Manchester, UK (s.hettiwatte@student.umist.ac.uk).
Zhongdong Wang is a Lecturer at UMIST (zhongdong.wang@umist.ac.uk).
Peter Crossley is a Reader at UMIST (p.crossley@umist.ac.uk).
Alan Darwin is Chief of Development, Alstom T&D Transformers, Stafford, UK (alan.darwin@tde.alstom.com).
Gwilym Edwards is a Senior Engineer at Edison Mission, Dinorwig Power Station, Llanberis, Gwynedd, UK (edwardsg@fhc.co.uk).

II. Test System

The experimental test system is shown in Fig.1. The PD signal is generated by a calibrator connected to one of the turns in the winding. The injected current and the resulting line and neutral-end currents are measured and stored in a computer. A capacitor is connected between the line-end and the earth to represent the effect of the capacitance of the bushing. The neutral-end is solidly connected to earth and the low voltage winding is short-circuited at earth potential.

A. Calibrator

The calibrator consists of a step wave generator (S) and a coupling capacitor (C_C) of 10pF. The rise time is <20ns and the repetition frequency is between 45 and 65Hz.

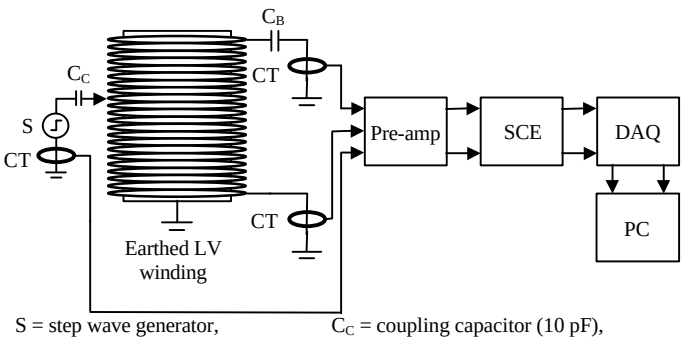

S = step wave generator, C_C = coupling capacitor (10 pF),
C_B = bushing capacitance (220 pF), SCE = Signal conditioning equipment,
CT = wide-band current transformers,
DAQ = Data acquisition and control, PC = Personal computer

Fig. 1. Experimental test system

B. Transformer winding

The 6.6kV winding is a continuous disc type design with 22 sections and 13 turns per section. The line-end terminal is connected to the 1st turn and the neutral-end terminal to the 286th turn (22sections x 13 turns). The dimensions of each turn is 2.5mm x 13.75mm and the thickness of insulation is 0.2mm. The inter-section distance is 4.5mm, the outer radius of the LV winding is 203.3mm and the inner and outer radii of the HV winding are 230mm and 267.7mm. The thickness of the pressboard between the LV and HV winding is 6mm.

0-7803-7322-7/02/$17.00 © 2002 IEEE

C. Measurement equipment

The measurement equipment consists of three wide-band current transformers (CTs), pre-amplifiers, a signal conditioning unit, the data acquisition and control system and the computer. The CTs measure the injected, line and neutral-end current signals and have a lower cut-off frequency (-3dB) of 50kHz and an upper cut-off frequency (-3dB) of 30MHz. The pre-amplifiers are used to amplify the signals measured by the CTs. Each pre-amplifier has a lower cut-off frequency (-3dB) of 22kHz, an upper cut-off frequency (-3dB) of 25MHz and remote automatic gain control (AGC) with steps of 0, 20, 40 and 60dB. The gain is independent of bandwidth. The signal conditioning equipment consist of selectable band pass filters (25kHz-500kHz, 25kHz-10MHz and 1MHz-10MHz), signal amplifiers, pre-amplifier gain control circuit and synchronised trigger circuit for the three signals. The data acquisition system (DAQ) is based on two dual channel National Instrument™ digital oscilloscope boards. Each channel has a bandwidth (-3dB) of 100MHz, a maximum single shot sampling rate of 100MS/s and 8-bit amplitude resolution. Once the digital oscilloscope cards have been triggered, 20ms of data is captured on all three channels and stored in buffer memory. This data is then transferred to the computer via a high-speed serial optical fibre link. In addition to its role in data capture, the DAQ also includes a digital input/output control system which determines the gain of the amplifiers and the choice of band-pass filter.

III. SIGNAL PROCESSING

A. Time domain signals

The signals captured by the data acquisition system when a pulse is injected into the 130th turn are shown in Fig.2. The upper trace is the injected signal, the middle the line-end signal and the lower the neutral-end signal. All the signals are sampled at 100MS/s and the band pass filter is set to 25kHz-10MHz. The figure shows that the duration of the injected current pulse is 100ns and the line and neutral-end signals differ from the injected signal in their wave shape.

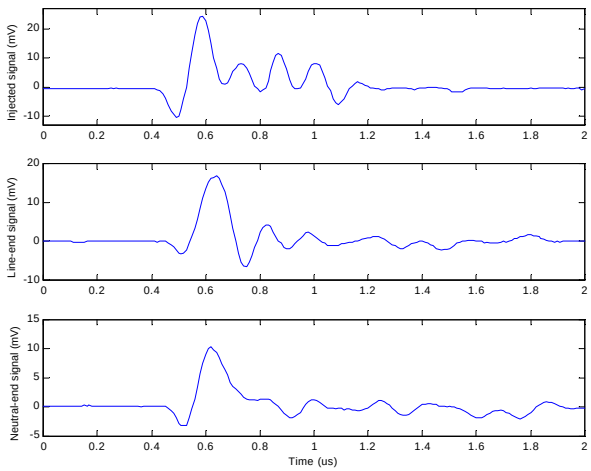

Fig. 2. Measured signals when calibrator is connected to 130th turn (Sampling rate: 100MS/s, and band pass filter: 25kHz - 10MHz)

An adaptive noise canceller, see Fig.3, was used to cancel the random noise in the measured current signals. The signal source produces the PD signal pulse and the noise source produces the random noise present in the measurements.

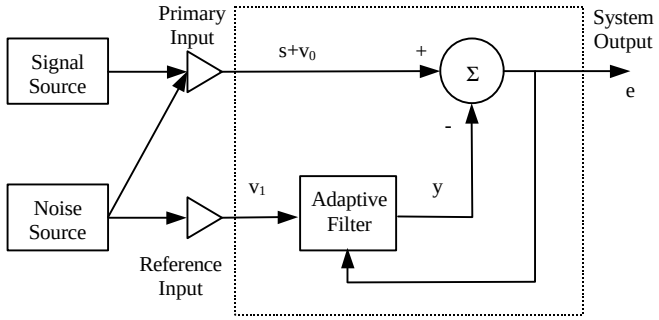

Adaptive Noise Canceller

Fig. 3. Adaptive noise cancelling filter

The primary input consists of the PD signal (s) with noise (v_0). The reference input contains noise (v_1), which is not correlated with the signal but correlated with the noise v_0 in an unknown way [3]. The filter output at k^{th} sampling instant is given by

$$y(k) = \sum_{i=0}^{N-1} w_i(k) v_1(k-i) \quad (1)$$

where N is the number of filter weights (w_i).

The system output is given by

$$e(k) = s(k) + v_0(k) - y(k) \quad (2)$$

Filter weights update according to the Least Mean Square (LMS) algorithm and are given by

$$w_i(k+1) = w_i(k) + 2\mu e(k) v_1(k-i) \quad (3)$$

where μ is a constant which governs the convergence of filter weights. When applied to the PD signals optimum results were obtained when N = 64 and μ = 0.1. The primary input was the PD signal with noise and the reference input was the noise measured before the PD signal was activated. The spectra obtained with adaptive filtering showed a definite improvement over those obtained without adaptive filtering.

To improve the frequency resolution of the spectra the truncated time domain signal samples were zero padded to a power of two before applying a fast Fourier transform (FFT). For example, when the time domain signal was sampled at 100MS/s, 8000 samples were collected and augmented with zeros until the total length was equal to 32768 (2^{15}) or 65536 (2^{16}) sample points. This helps to achieve about 3kHz or 1.5kHz frequency resolution in the spectra. A power of two was selected to improve the speed of FFT process. The frequency spectra obtained for the time domain signals in Fig. 2, with 8000 signal samples zero padded to 32768 samples, is shown in Fig. 4.

B. Frequency spectra

The frequency spectra of the time domain signals were obtained by applying an FFT after appropriate zero padding.

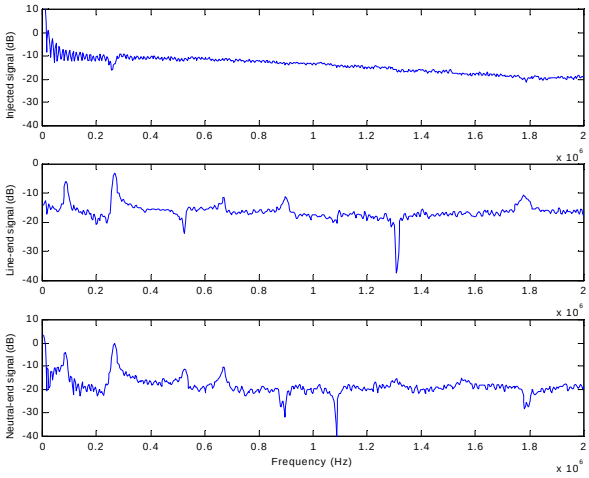

Fig. 4. Frequency spectra of measured signals for turn no. 130. No. of samples =8000, zero padded to 32768 samples.

Fig.4 indicates that the injected PD signal has a reasonably flat spectrum over a frequency range of 0 to 2 MHz, whilst the spectra of the measured signals at the line and neutral ends contain numerous crests and troughs caused by the propagation path of the pulse.

Similar time domain signals and their associated spectra were obtained for PDs injected at different turns along the winding. The spectra of the line-end signals are shown in Fig. 5, while those from the simulations are in Fig. 6.

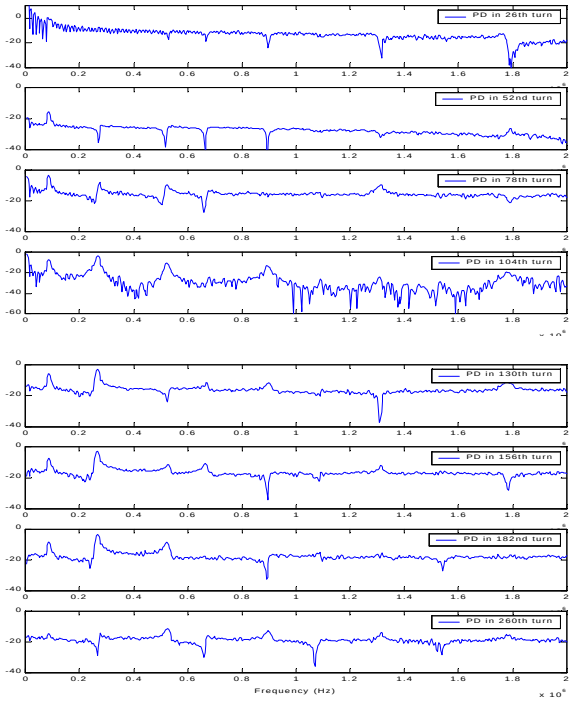

Fig. 5. Frequency spectra of measured signals at line-end (in dB) (Sampling rate: 100 MS/s, and band pass filter: 25 kHz - 10 MHz)

The spectra of the neutral-end signals are shown in Fig.7 and corresponding results from the simulations are in Fig.8. It can be seen that the crests in the spectra are at fixed frequencies and are not affected by the location of the injected PD pulse.

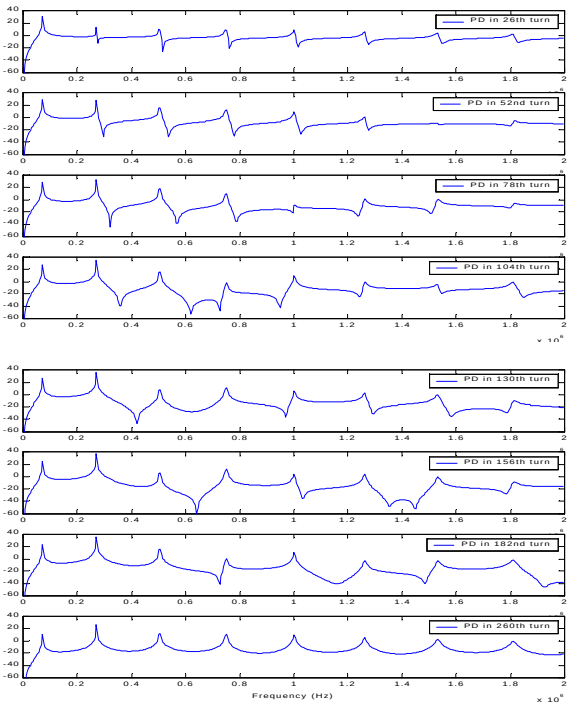

Fig. 6. Frequency spectra of line-end signals from simulation (in dB)

The locations of the poles in the measured spectra are listed in Table 1 and those generated by the simulation model in Table 2.

TABLE 1 POSITION OF MEASURED POLES (KHZ)

p_1	p_2	p_3	p_4	p_5	p_6	p_7	p_8
85	272	522	665	897	1086	1303	1770

TABLE 2 POSITION OF SIMULATED POLES (KHZ)

P_1	p_2	p_3	p_4	p_5	p_6	p_7	p_8
70	271	508	753	1005	1265	1534	1813

The first three poles in the measurement results occur at frequencies approximately equal to those generated by the simulator. However, higher order poles are at frequencies lower than the simulator predicted. Possible reasons will be discussed later in the paper.

It can be also seen that the zeros in the line-end spectra increase in frequency as the PD source moves away from the line-end, whereas the zeros in the neutral-end spectra decrease in frequency. This again helps confirm the validity of the simulation results.

One notable feature with the measurement results is that when the PD pulse was injected close to the line-end (turn no. 26) the poles in the line-end signal spectra disappear. Similarly, the magnitudes of the poles in the simulated results for a PD at turn 26 are very small compared with those for a PD further down the winding. The reason can be explained as follows:- the injected signal, which has frequency components at the pole frequencies, has two paths to propagate; one is

through the bushing capacitance to ground and the other through the neutral terminal to ground.

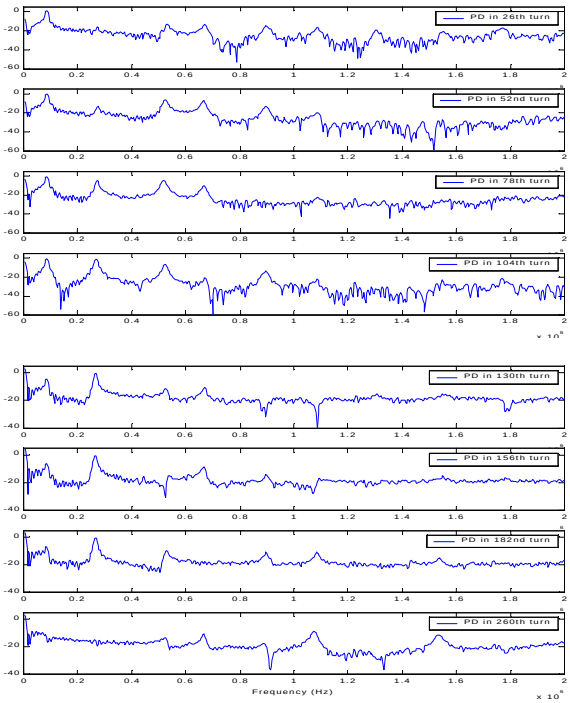

Fig. 7. Frequency spectra of measured signals at neutral-end (in dB) (Sampling rate: 100MS/s, and band pass filter: 25kHz - 10MHz)

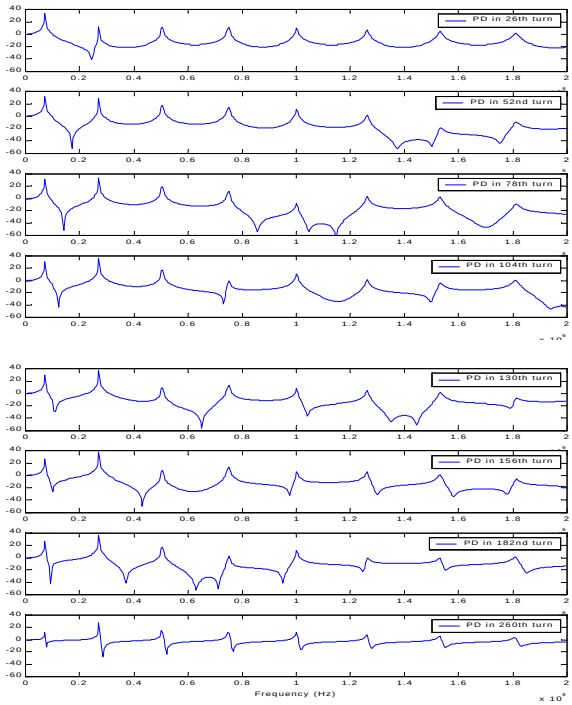

Fig. 8. Frequency spectra of neutral-end signals from simulation (in dB)

When the injection point is close to the line-end, the current avoids the high impedance path of the bushing capacitor and travels through the winding to the grounded neutral. Consequently, the magnitude of the poles, particularly those that represent low frequency resonances, decreases in value at the line-end. Due to the inadequate vertical resolution of the data acquisition system (DAQ) the poles in the line-end current become undetectable as the PD source approaches the line-end.

To investigate the effect of vertical resolution on the magnitude of the poles and zeros in the spectra, the time domain signals generated when the calibrator is connected to the 130th turn were band-limited by a 4thorder 25kHz-500kHz pass-band filter. The original signals, without band-pass filtering, are shown in Fig.2 (time axis: 0-2μs) and the band-pass filtered signals in Fig.9 (time axis: 0 - 80μs).

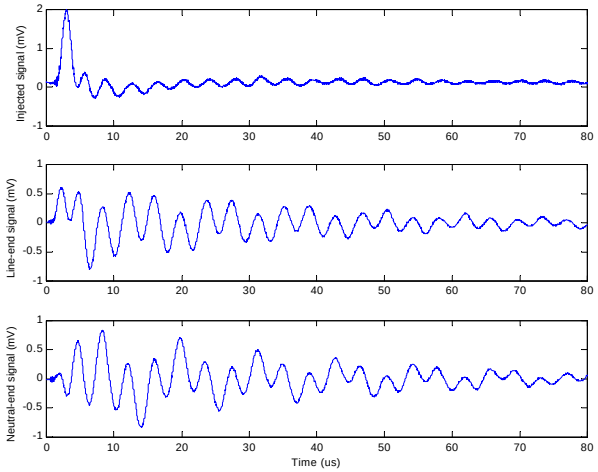

Fig.9. Measured signals when calibrator is connected to 130th turn (Sampling rate: 100MS/s, and band pass filter: 25kHz – 500kHz)

In Fig.9, the high frequency components in the current signals has been blocked by the filter and therefore the 8-bit capability of the DAQ system is more fully utilised in digitising the lower frequency components that are used to locate the source of the discharge. The spectra of the line and neutral-end band-limited signals are shown in Fig.10 and Fig.11 with a frequency axis from 0 – 500kHz. The vertical resolution is now more defined and the poles are clearly visible. This improvement in resolution is particularly noticeable when the source of the PD is near the line-end (e.g. 26th turn) and the location of the low frequency poles in the line-end band-pass filtered signals (Fig.10) are compared with the corresponding unfiltered signals in Fig.5.

The positions of poles p1 and p2 in the spectra of the line and neutral-end band-pass filtered signals are at 85kHz and 272kHz respectively. This is identical to that observed with the 10MHz system, where the results are presented in Table 1 and the spectra are shown in Fig.5 and Fig.7. The position of zeros obtained from the measured band-pass filtered signals and the corresponding values generated by the simulator are listed in Table 3 and Table 4.

TABLE 3 POSITION OF ZEROS IN LINE-END SIGNALS (25 ~ 500 KHZ)

PD (turn no.)	Measurements	Simulation
	z_1 (kHz)	z_1 (kHz)
26	243	275
52	290	295
78	339	321
104	-	358
130	-	419
156	-	-
182	-	-
260	-	-

TABLE 4 POSITION OF ZEROS IN NEUTRAL-END SIGNALS (25 ~ 500KHZ)

PD (turn no.)	Measurements	Simulation
	z_1 (kHz)	z_1 (kHz)
26	-	244
52	235	172
78	168	141
104	165	122
130	150	109
156	143	99
182	119	91
260	92	74

Although some zeros in the line-end signals are undetectable, the neutral-end signal shows that the frequency location of the zeros in the spectra decrease as the PD injection point moves away from the line-end.

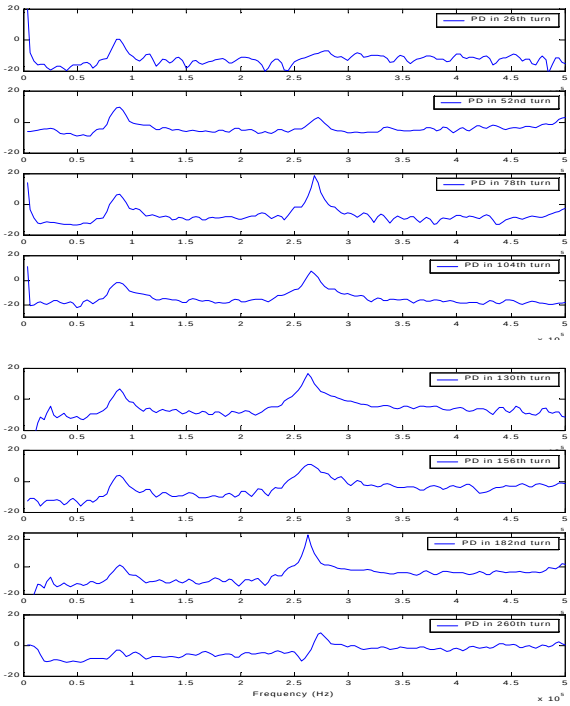

Fig. 10. Frequency spectra of measured signals at line-end (in dB) (Sampling rate: 100MS/s, and band pass filter: 25kHz – 500kHz)

To investigate the effect of sampling frequency on measured signals, the sampling rate of the DAQ system was reduced to 20MS/s and all other parameters were kept constant. The positions of zeros in the measured and simulated spectra are listed in Table 5 and Table 6.

TABLE 5 POSITION OF ZEROS (Z) IN LINE-END SIGNALS (25 ~ 500 KHZ)

PD (turn no.)	Measurements	Simulation
	z_1 (kHz)	z_1 (kHz)
26	287	275
52	306	295
78	333	321
104	382	358
130	438	419
156	-	-
182	-	-
260	-	-

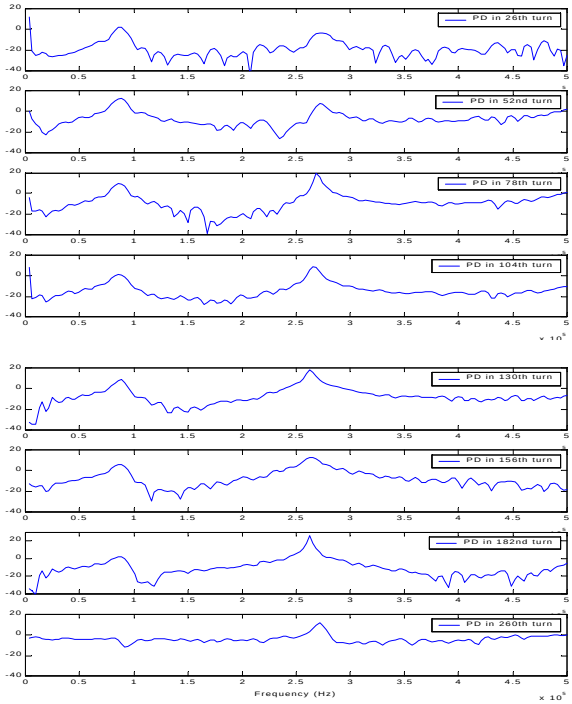

Fig. 11. Frequency spectra of measured signals at neutral-end (in dB) (Sampling rate: 100 MS/s, and band pass filter: 25 kHz – 500kHz)

TABLE 6 POSITION OF ZEROS (Z) OF NEUTRAL-END SIGNALS (25 ~ 500 KHZ)

PD (turn no.)	Measurements	Simulation
	z_1 (kHz)	z_1 (kHz)
26	226	244
52	164	172
78	148	141
104	100	122
130	104	109
156	98	99
182	-	91
260	-	74

Although the last few zeros in the measured results in Table 5 were not detected, a clear pattern exists which indicates that the frequency location of the first zero in each line-end spectra increases as the position of the injected PD pulse is moved along the winding from the line-end to the neutral; i.e. the frequency increases in proportion to the turn number.

Similarly, the last few zeros were not detected in the measured results in Table 6, but again a clear pattern exists:- the frequency location of the first zero in each neutral-end spectra decreases as the position of the injected PD pulse is moved along the winding from the line-end to the neutral.

The results obtained at a sampling rate of 20MS/s are closer to those predicted by the simulation model, than those obtained at 100MS/s. This indicates that the assumptions made in designing the simulator are valid at frequencies up to 500kHz, but limitations exist at higher frequencies.

IV. CONCLUSION

Experimental investigation into the propagation behaviour of partial discharge pulses in a continuous disc type transformer winding was described. Measured results were used to validate a simulation model of the winding based on multi-conductor transmission line theory. The current signals measured at the line and neutral-end terminals during experimental and simulated studies were converted into frequency spectra and these were analysed to locate the poles and zeros. The location of the low-order zeros in the line-end signal increase in frequency as the source of the discharge moves along the winding from the line-end to the neutral-end. Conversely, the locations of the zeros in the neutral spectra decrease in frequency. The poles are not affected by the location of the discharge but do depend on the characteristics of the winding. Consequently, the poles in the measured spectra can be used to validate the simulation model. Once validated, the zeros in the spectra generated by the simulation model for a discharge at a known location in the winding can be compared with the zeros in the measured spectra. If the frequency locations match the point of simulated discharge can be considered as the point of discharge on the real winding. If the locations differ the comparison process is repeated with a simulated discharge at a different location.

The frequency spectra of the line-end terminal signals are affected by the bushing capacitance which blocks most of the low frequencies present in the signal when the PD pulse is injected close to the line-end terminal. This means that the zeros in the measured line-end signals are difficult to detect when the source of the discharge is near the line-end terminal. Further work is required to determine the limitations and accuracy of the PD location technique particularly when one considers the impact of noise, the DAQ sampling frequency, the bandwidth and resolution of the signal conditioning system and the bushing capacitance at the line terminal.

V. ACKNOWLEDGEMENT

The authors would like to thank Alstom, Edison Mission, the National Grid Company and UMIST for permission to publish the paper. They especially thank Dr. Y. Tu for constructing the PD measurement system and for his assistance with the experimental tests.

VI. REFERENCES

Papers from Conference Proceedings (Unpublished):

[1] S. N. Hettiwatte, P. A. Crossley, Z. D. Wang, A. Darwin and G. Edwards, 'Simulation of a transformer winding for partial discharge propagation studies', submitted to IEEE Power Engineering Society Winter Meeting 2002, New York, USA.

Papers from Conference Proceedings (Published):

[2] Z. D. Wang, P. A. Crossley and K. J. Cornick, 'Partial discharge location in power transformers using the spectra of the terminal current signals', Proceedings of the 11th International Symposium on High Voltage Engineering (ISH-99), August 1999, London, UK.

Books:

[3] B. Widrow and S. D. Stearns, 'Adaptive signal processing', New Jersey: Prentice-Hall, 1985, pp 304.

VII. BIOGRAPHIES

Sujeewa Hettiwatte was born in Colombo, Sri Lanka, on 2 September 1968. He received his BSc (Eng) degree with 1st class honours and MEng degree, both in electronic and telecommunication engineering from the University of Moratuwa, Sri Lanka, in 1994 and 2000. He is a Lecturer in Electrical and Computer Engineering at the Open University of Sri Lanka and studying for his PhD on partial discharge location in transformers. His research mainly focuses on computer simulation and signal processing aspects of the project.

Zhongdong Wang was born in Hebei, China, on 19 January 1969. She received her BSc and MSc degrees in electrical engineering at Tsinghua University in 1991 and 1993. She completed her PhD at UMIST in 1999 and subsequently joined UMIST as a Lecturer. Her research interests are in partial discharge monitoring in transformers and cables, fast transient distribution in windings, detection of winding displacements and ageing of insulation.

Peter Crossley was born in Burnley, England, on 25 June 1956. He graduated with a BSc degree from UMIST and a PhD degree from the University of Cambridge in 1983. During the period 1977 – 1990, he was employed by GEC and GEC Alstom on the design and application of digital protection relays. In 1991 he joined UMIST where he is a Reader in Power Systems. His research interests are in power system protection and condition monitoring. He has published more than 120 technical papers and is a joint author of a book on embedded generation.

Alan Darwin was born in Woodford, England, on 19 October 1945. He graduated with a BSc (Eng) degree in electrical engineering from Southampton University in 1967. He joined English Electric (later GEC, GEC Alsthom and presently ALSTOM T&D Ltd Transformers) at Stafford in 1967 as a graduate trainee and joined the HV transformer design department in 1969. He has subsequently worked in the design department as Chief Designer, Chief Engineer and Chief Transformer Engineer. At present, he is Chief of Development. He is a Member of the IEE and a Senior Member of the IEEE.

Gwilym Edwards was born in Bangor, Wales, on 25 May 1961. He started his working life as an electrical craft apprentice with Babcock & Wilcox, working on a number of power stations throughout the UK. He joined the CEGB in 1986 at Dinorwig Power Station as an electrical craftsman. He subsequently received a HND in Engineering at Gwynedd College. Since 1990 he has worked as an electrical engineer in the Engineering Development Department for Edison Mission Energy First Hydro Company, responsible for generator motor rotors, transformers and 400kV plant.